J|A|C|S
ARTICLES
Published on Web 10/06/2007

Activation of Carbon−Hydrogen Bonds via 1,2-Addition across M−X (X = OH or NH_2) Bonds of d^6 Transition Metals as a Potential Key Step in Hydrocarbon Functionalization: A Computational Study

Thomas R. Cundari,*,† Thomas V. Grimes,† and T. Brent Gunnoe*,‡

Contribution from the Department of Chemistry and Center for Advanced Scientific Computing and Modeling (CASCaM), University of North Texas, P.O. Box 305070, Denton, Texas 76203-5070, and Department of Chemistry, North Carolina State University, Raleigh, North Carolina 27695-8204

Received June 6, 2007; E-mail: tomc@unt.edu

Abstract: Recent reports of 1,2-addition of C−H bonds across Ru−X (X = amido, hydroxo) bonds of TpRu(PMe$_3$)X fragments {Tp = hydridotris(pyrazolyl)borate} suggest opportunities for the development of new catalytic cycles for hydrocarbon functionalization. In order to enhance understanding of these transformations, computational examinations of the efficacy of model d^6 transition metal complexes of the form [(Tab)M(PH$_3$)$_2$X]^q (Tab = *tris*-azo-borate; X = OH, NH_2; $q = -1$ to $+2$; M = Tc^I, Re^I, Ru^{II}, Co^{III}, Ir^{III}, Ni^{IV}, Pt^{IV}) for the activation of benzene C−H bonds, as well as the potential for their incorporation into catalytic functionalization cycles, are presented. For the benzene C−H activation reaction steps, kite-shaped transition states were located and found to have relatively little metal−hydrogen interaction. The C−H activation process is best described as a metal-mediated proton transfer in which the metal center and ligand X function as an activating electrophile and intramolecular base, respectively. While the metal plays a primary role in controlling the kinetics and thermodynamics of the reaction coordinate for C−H activation/functionalization, the ligand X also influences the energetics. On the basis of three thermodynamic criteria characterizing salient energetic aspects of the proposed catalytic cycle and the detailed computational studies reported herein, late transition metal complexes (e.g., Pt, Co, etc.) in the d^6 electron configuration {especially the TabCo(PH$_3$)$_2$(OH)$^+$ complex and related Co(III) systems} are predicted to be the most promising for further catalyst investigation.

1. Introduction

The development of catalysts for the functionalization of carbon−hydrogen bonds is an important pursuit that could impact both commodity and fine chemical markets. Transition metal systems that initiate stoichiometric metal-mediated activation of carbon−hydrogen bonds are known,[1] and many of these systems function at ambient conditions. The most commonly invoked mechanisms for the C−H bond cleavage step include oxidative addition (OA), σ-bond metathesis (SBM), and electrophilic substitution (ES). Despite the success of metal-mediated C−H activation, the incorporation of stoichiometric C−H activations into catalytic cycles remains relatively rare,[2] and this is especially true for the functionalization of aliphatic hydrocarbons. Noteworthy examples of catalytic conversions include alkane dehydrogenation,[3−5] alkane metathesis,[6] alkane silylation,[7] alkane borylation,[8] as well as hydrocarbon functionalization by Shilov-type metal electrophiles.[9] In an interesting tandem synthesis, Vedernikov and Caulton have coupled alkane dehydrogenation with aziridination of the resultant olefins.[10]

† University of North Texas.
‡ North Carolina State University.

(1) (a) Labinger, J. A.; Bercaw, J. E. *Nature* **2002**, *417*, 507. (b) Arndtsen, B. A.; Bergman, R. G.; Mobley, T. A.; Peterson, T. H. *Acc. Chem. Res.* **1995**, *28*, 154. (c) Jones, W. D.; Feher, F. J. *Acc. Chem. Res.* **1989**, *22*, 91. (d) Crabtree, R. H. *Chem. Rev.* **1985**, *85*, 245. (e) Crabtree, R. H. *Chem. Rev.* **1995**, *95*, 987. (f) *Activation and Functionalization of C-H Bonds*; Goldberg, K. I., Goldman, A. S., Eds.; ACS Symposium Series 885; American Chemical Society: Washington, DC, 2004. (g) Guari, Y.; Sabo-Etienne, S.; Chaudret, B. *Eur. J. Inorg. Chem.* **1999**, 1047. (h) Jones, W. D. *Acc. Chem. Res.* **2003**, *36*, 140.

(2) (a) Sen, A. *Acc. Chem. Res.* **1998**, *31*, 550. (b) Crabtree, R. H. *J. Chem. Soc., Dalton Trans.* **2001**, 2437. (c) Periana, R. A.; Bhalla, G.; Tenn, W. J., III; Young, K. J. H.; Liu, X. Y.; Mironov, O.; Jones, C. J.; Ziatdinov, V. R. *J. Mol. Catal. A* **2004**, *220*, 7. (d) Goj, L. A.; Gunnoe, T. B. *Curr. Org. Chem.* **2005**, *9*, 671. (e) Ritleng, V.; Sirlin, C.; Pfeffer, M. *Chem. Rev.* **2002**, *102*, 1731. (f) Dyker, G. *Angew. Chem., Int. Ed.* **1999**, *38*, 1698.

(3) (a) Belli, J.; Jensen, C. M. *Organometallics* **1996**, *15*, 1532. (b) Zhu, K.; Achord, P. D.; Zhang, X.; Krogh-Jespersen, K.; Goldman, A. S. *J. Am. Chem. Soc.* **2004**, *126*, 13044. (c) Renkema, K. B.; Kissin, Y. V.; Goldman, A. S. *J. Am. Chem. Soc.* **2003**, *125*, 7770. (d) Krogh-Jespersen, K.; Czerw, M.; Summa, N.; Renkema, K. B.; Achord, P. D.; Goldman, A. S. *J. Am. Chem. Soc.* **2002**, *124*, 11404. (e) Kanzelberger, M.; Singh, B.; Czerw, M.; Krogh-Jespersen, K.; Goldman, A. S. *J. Am. Chem. Soc.* **2000**, *122*, 11017. (f) Liu, F.; Pak, E. B.; Singh, B.; Jensen, C. M.; Goldman, A. S. *J. Am. Chem. Soc.* **1999**, *121*, 4086.

(4) Liu, F.; Pak, E. B.; Singh, B.; Jensen, C. M.; Goldman, A. S. *J. Am. Chem. Soc.* **1999**, *121*, 4086.

(5) Renkema, K. B.; Kissin, Y. V.; Goldman, A. S. *J. Am. Chem. Soc.* **2003**, *125*, 7770.

(6) Goldman, A. S.; Roy, A. H.; Huang, Z.; Ahuja, R.; Schinski, W.; Brookhart, M. *Science* **2006**, *312*, 257.

(7) (a) Sadow, A. D.; Tilley, T. D. Presented at the 224th National Meeting of the American Chemical Society, Boston, MA, August 18−22, 2002; Abstract INOR-563. (b) Sadow, A. D.; Tilley, T. D. *J. Am. Chem. Soc.* **2005**, *127*, 643.

10.1021/ja074125g CCC: $37.00

Scheme 1. Oxidative Addition (OA) and σ-Bond Metathesis (SBM) Mechanisms for C−H Bond Activation; q Denotes the Formal Oxidation State of the Metal

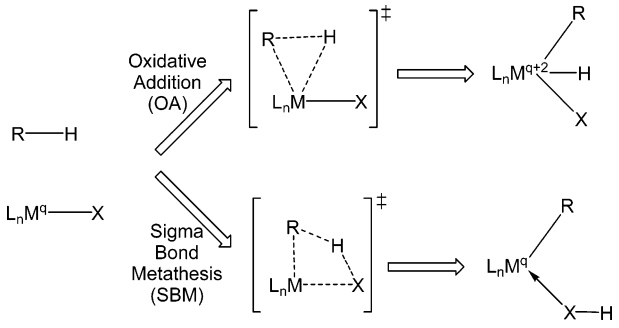

In the typical OA mechanism, both the carbon and hydrogen of the C−H bond that is cleaved are transferred to a low-valent transition metal center via a three-centered transition state, Scheme 1.[11] In contrast to the three-center transition state associated with OA, SBM is a concerted reaction involving four atomic centers including the metal center, the ligand that receives the transferred proton, and the C and H atoms of the bond being activated, Scheme 1. The SBM pathway leaves the formal oxidation state of the metal center unchanged. Cundari has contrasted OA and SBM pathways of carbon−hydrogen bond activation in terms of metal complex to substrate electron donation and backdonation.[12] Both OA and SBM are characterized by an "electrophilic" phase with dominant substrate to metal donation early (i.e., before the transition state) in the reaction coordinate. A "nucleophilic" phase dominated by metal complex to substrate backdonation follows and serves to delineate the mechanisms.[12] In typical (i.e., monometallic complex) OA pathways, the metal acts as both electrophile and nucleophile, and thus both ends of the C−H bond being activated end up on the metal. For SBM systems, the donor orbital on the metal complex is a metal−ligand frontier orbital polarized toward the more electronegative ligand. Periana and Goddard et al. have proposed an oxidative-hydrogen migration (OHM) mechanism for C−H activation by Ir(III) complexes as a variant of OA and SBM.[13] The OHM transition state is in some respects intermediate between OA and SBM[14] transition states (see below) and is distinguished from the latter by more significant interaction between the metal and the hydrogen of the carbon−hydrogen bond being activated. The distinction between OA, OHM, and SBM is reminiscent of many debates in chemical bonding; while technical distinctions exist and demarcation into categories can be useful, real mechanisms may lie on a spectrum defined by these three classifications.

Scheme 2. Possible Routes for Catalytic C−H Functionalization That Involve Net 1,2-Addition of C−H Bonds across M−X(R) Bonds (X = O or NR)

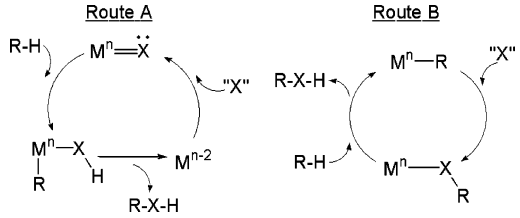

In addition to OA, SBM, and ES pathways for C−H activation, the net 1,2-addition of C−H bonds across M−X (X = heteroatomic ligand such as amido, alkoxo, imido, oxo, etc.) bonds also holds promise as a step in overall catalytic C−H functionalization.[15] Only a few examples of net 1,2-addition of C−H bonds across M−X bonds have been reported. For example, the Wolczanski[16] and Bergman[17] groups have studied the 1,2-addition of C−H bonds, including that of methane for the former group, across d^0 metal−imido (M = NR) bonds of early transition metals such as Ti and Zr. It has been established that the reaction is an overall $[2_\sigma + 2_\pi]$ addition and that the transition state has a four-centered arrangement preceded by an alkane or arene adduct. The resulting alkyl/aryl product is only a single C−N reductive elimination step away from substrate functionalization to produce amine. However, reductive elimination is difficult for electropositive early transition metal complexes. In contrast, precedent for C−N and C−O reductive elimination from late transition metals is extensive.[18] Thus, extension of the net 1,2-addition of C−H bonds to late transition metal systems might ultimately be incorporated into catalytic cycles for C−H functionalization.

(8) (a) Chen, H.; Schlecht, S.; Semple, T. C.; Hartwig, J. F. *Science* **2000**, *287*, 1995. (b) Webster, C. E.; Fan, Y.; Hall, M. B.; Kunz, D.; Hartwig, J. F. *J. Am. Chem. Soc.* **2003**, *125*, 858.
(9) (a) Periana, R. A.; Taube, D. J.; Gamble, S.; Taube, H.; Satoh, T.; Fujii, H. *Science* **1998**, *280*, 560. (b) Periana, R. A.; Taube, D. J.; Evitt, E. R.; Loffler, D. G.; Wentrcek, P. R.; Voss, G.; Masuda, T. *Science* **1993**, *253*, 340. (c) Shilov, A. E.; Shul'pin, G. B. *Chem. Rev.* **1997**, *97*, 2879. (d) Lin, M.; Chen, S.; Garcia-Zayas, E. A.; Sen, A. *J. Am. Chem. Soc.* **2001**, *123*, 1000. (e) Jones, C. J.; Taube, D. J.; Ziatdinov, V. R.; Periana, R. A.; Nielsen, R. J.; Oxgaard, J.; Goddard, W. A., III. *Angew. Chem., Int. Ed.* **2004**, *43*, 4626. (f) Xu, X.; Fu, G.; Goddard, W. A., III; Periana, R. A. *Stud. Surf. Sci. Catal.* **2004**, *147*, 499. (g) Stahl, S.; Labinger, J. A.; Bercaw, J. E. *Angew. Chem., Int. Ed.* **1998**, *37*, 2181. (h) Shilov, A. E.; Shteinman, A. A. *Acc. Chem. Res.* **1999**, *32*, 763. (i) Periana, R. A.; Ortmann, D. A.; Dagmara, A.; Mironov, O. A. Presented at the 224th National Meeting of the American Chemical Society, Boston, MA, August 18−22, 2002; Abstract INOR-465. (j) Kua, J.; Xu, X.; Periana, R. A.; Goddard, W. A., III. *Organometallics* **2002**, *21*, 511. (k) Periana, R. A.; Ortmann, D. A. Presented at the 223rd National Meeting of the American Chemical Society, Orlando, FL, April 7−11, 2002; Abstract INOR-157.
(10) Vedernikov, A. N.; Caulton, K. G. *Chem. Commun.* **2004**, *2*, 162.
(11) (a) Jones, W. D. *Acc. Chem. Res.* **2003**, *36*, 140. (b) Jones, W. D.; Feher, F. J. *Acc. Chem. Res.* **1989**, *22*, 91.
(12) Cundari, T. R. *J. Am. Chem. Soc.* **1994**, *116*, 340.
(13) Oxgaard, J.; Muller, R. P.; Goddard, W. A., III; Periana, R. A. *J. Am. Chem. Soc.* **2004**, *126*, 352.
(14) (a) Thompson, M. E.; Baxter, S. M.; Bulls, A. R.; Burger, B. J.; Nolan, M. C.; Santarsiero, B. D.; Schaefer, W. P.; Bercaw, J. E. *J. Am. Chem. Soc.* **1987**, *109*, 203. (b) Lam, W. H.; Jia, G.; Lin, Z.; Lau, C. P.; Eisenstein, O. *Chem. Eur. J.* **2003**, *9*, 2775.
(15) (a) Tenn, W. J., III; Young, K. J. H.; Bhalla, G.; Oxgaard, J.; Goddard, W. A., III; Periana, R. A. *J. Am. Chem. Soc.* **2005**, *127*, 14172. (b) Feng, Y.; Lail, M.; Barakat, K. A.; Cundari, T. R.; Gunnoe, T. B.; Petersen, J. L. *J. Am. Chem. Soc.* **2005**, *127*, 14174. (c) Feng, Y.; Lail, M.; Foley, N. A.; Gunnoe, T. B.; Barakat, K. A.; Cundari, T. R.; Petersen, J. L. *J. Am. Chem. Soc.* **2006**, *128*, 7982.
(16) (a) Cummins, C. C.; Baxter, S. M.; Wolczanski, P. T. *J. Am. Chem. Soc.* **1988**, *110*, 8731. (b) Cummins, C. C.; Schaller, C. P.; Van Duyne, G. D.; Wolczanski, P. T.; Chan, A. W. E.; Hoffmann, R. *J. Am. Chem. Soc.* **1991**, *113*, 2985. (c) Schaller, C. P.; Wolczanski, P. T. *Inorg. Chem.* **1993**, *32*, 131. (d) Bennett, J. L.; Wolczanski, P. T. *J. Am. Chem. Soc.* **1994**, *116*, 2179. (e) Schaller, C. P.; Bonanno, J. B.; Wolczanski, P. T. *J. Am. Chem. Soc.* **1994**, *116*, 4133. (f) Schaller, C. P.; Cummins, C. C.; Wolczanski, P. T. *J. Am. Chem. Soc.* **1996**, *118*, 591. (g) Bennett, J. L.; Wolczanski, P. T. *J. Am. Chem. Soc.* **1997**, *119*, 10696. (h) Schafer, D. F., II; Wolczanski, P. T. *J. Am. Chem. Soc.* **1998**, *120*, 4881. (i) Slaughter, L. M.; Wolczanski, P. T.; Klinckman, T. R.; Cundari, T. R. *J. Am. Chem. Soc.* **2000**, *122*, 7953. (j) Cundari, T. R.; Klinckman, T. R.; Wolczanski, P. T. *J. Am. Chem. Soc.* **2002**, *124*, 1481. (k) Cundari, T. R. *J. Am. Chem. Soc.* **1992**, *114*, 10557.
(17) (a) Hoyt, H. M.; Michael, F. E.; Bergman, R. G. *J. Am. Chem. Soc.* **2004**, *126*, 1018. (b) Walsh, P. J.; Hollander, F. J.; Bergman, R. G. *J. Am. Chem. Soc.* **1988**, *110*, 8729.
(18) The proclivity of late transition metals for C−O and C−N has been profitably exploited in, for example, the well-known Hartwig−Buchwald etheration and amination reactions. (a) Reductive: Stuermer, R. In *Organic Synthesis Highlights V*; Schmalz,; H.-G., Wirth, T., Eds.; Wiley-VCH: New York, 2003; p 22. (b) Muci, A. R.; Buchwald, S. L. *Top. Curr. Chem.* **2002**, *219*, 131. (c) Hartwig, J. F. In *Comprehensive Coordination Chemistry II: From Biology to Nanotechnology*; McCleverty, J. A., Meyer, T. J., Eds.; Elsevier: New York, Amsterdam, 2004; Vol. 9, p 369.

Scheme 2 shows two pathways in which 1,2-addition of C−H bonds across M−X (X = O or NR) or M−XR bonds could be incorporated into a catalytic cycle. Route A involves the 1,2-addition of a C−H bond across a metal−heteroatom (M═X) bond, which is followed by reductive elimination of functionalized product (R−X−H). Regeneration of the active species occurs via an atom- or group-transfer reagent. This route is perhaps similar in some respects to metal-catalyzed insertion of carbenes into C−H bonds.[19] Route B involves the initial functionalization of a metal−alkyl moiety via formal insertion of an oxygen atom or nitrene fragment into a metal−alkyl or metal−aryl bond. Hydrogen transfer from a hydrocarbon substrate follows to make the functionalized product and regenerate the active metal−alkyl species. Mayer and Brown have reported high-valent Re−oxo complexes that undergo oxo insertion into Re−Ph bonds under photolytic and thermal conditions.[20] In addition, Periana et al. have recently reported remarkably facile conversions of the Re−Me bond of methylrheniumtrioxo to a methoxo ligand upon treatment with various oxidants,[21] with preliminary mechanistic studies suggesting that the inserted oxygen atom is not derived from a Re═O ligand.

Recently, our groups have become interested in extending 1,2-addition of C−H bonds across M−X bonds to *late* transition metals in relatively *low* oxidation states. While *high* valent late-(r) transition metal−oxo and hydroxo/alkoxo complexes are prevalent in the functionalization of C−H bonds, these systems typically activate C−H bonds through net radical hydrogen-atom abstraction routes for which the metal center does not directly interact with the C−H bond, but rather, the metal serves as an oxidizing "electron reservoir."[22−24] Our working hypothesis is that lower oxidation states increase the propensity toward even-electron processes such as intermolecular heterolytic C−H bond cleavage and intramolecular 1,2-addition reactions (Scheme 3).[25] For example, it has been demonstrated that coordinatively and electronically saturated octahedral Ru(II) and Fe(II) amido complexes can deprotonate (i.e., an even-electron transformation) relatively acidic C−H bonds including those of phenylacetylene, 1,4-cyclohexadiene, and triphenylmethane. In one prominent study, Bergman et al. investigated the reactivity of *trans*-$(dmpe)_2Ru(H)(NH_2)$ toward acidic C−H bonds.[26] Even very weakly acidic compounds such as toluene react, though the reaction is endothermic.[26] The corresponding Fe(II) analogue shows similar reactivity, although it is less basic than the ruthenium complex.[27] $TpRuL_2X$ (X = NHR, OR; Tp = hydrido-*tris*(pyrazolyl)borate) and (PCP)Ru(L)(NHR) (PCP = *bis*-phosphine "pincer" ligand) systems exhibit similar reactivity.[28−30] It is important to emphasize that these transformations likely involve *inter*molecular C−H bond cleavage without direct metal−CH interaction (Scheme 3).

Scheme 3. Three Pathways to Cleave C−H Bonds by Transition Metal Systems with Formally Anionic Heteroatomic Ligands

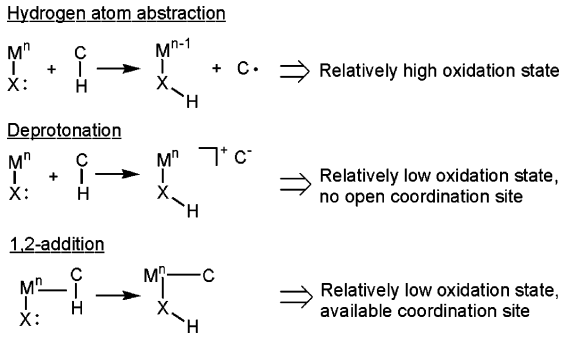

As we have previously suggested for reactions of (PCP)Ru(CO)NH_2,[29] the coordination of C−H bonds to similar systems[26,27] (i.e., amido, hydroxo, or related complexes in low oxidation states) could activate them toward a net intramolecular deprotonation by the highly basic non-dative ligand "X" (Scheme 3). We have reported evidence for such reactions with $TpRu(PMe_3)X$ (X = OH, OPh, or NHPh) systems,[15b,c] and Periana et al. have directly observed related reactions with an Ir(III)−methoxo complex.[15a,31] To our knowledge, these reports are the only examples of 1,2-addition of C−H bonds across M−X (X = OR, NHR, O, or NR) bonds for late transition metals in low oxidation states. In related chemistry, Macgregor et al. have reported the possible involvement of an Ir−acetate

(19) (a) Braga, A. A. C.; Maseras, F.; Urbano, J.; Caballero, A.; Mar Diaz-Requejo, M.; Perez, P. J. *Organometallics* **2006**, *25*, 5292. (b) de Fremont, P.; Stevens, E. D.; Fructos, M. R.; Mar Diaz-Requejo, M.; Perez, P. J.; Nolan, S. P. *Chem. Commun.* **2006**, *19*, 2045. (c) Doyle, M. P. *J. Org. Chem.* **2006**, *71*, 9253. (d) Doyle, M. P. *Top. Organomet. Chem.* **2004**, 203.
(20) Brown, S. N.; Mayer, J. M. *J. Am. Chem. Soc.* **1996**, *118*, 12119; Brown, S. N.; Mayer, J. M. *Organometallics* **1995**, *14*, 2951; Brown, S. N.; Mayer, J. M. *J. Am. Chem. Soc.* **1994**, *116*, 2219.
(21) Conley, B. L.; Ganesh, S. K.; Gonzales, J. M.; Tenn, W. J., III; Young, K. J. H.; Oxgaard, J.; Goddard, W. A., III; Periana, R. A. *J. Am. Chem. Soc.* **2006**, *128*, 9018.
(22) (a) Mayer, J. M. *Acc. Chem. Res.* **1998**, *31*, 441. (b) Bryant, J. R.; Taves, J. E.; Mayer, J. M. *Inorg. Chem.* **2002**, *41*, 2769. (c) Larsen, A. S.; Wang, K.; Lockwood, M. A.; Rice, G. L.; Won, T. J.; Lovell, S.; Sadílek, M.; Tureček, F.; Mayer, J. M. *J. Am. Chem. Soc.* **2002**, *124*, 10113. (d) Jonas, R. T.; Stack, T. D. P. *J. Am. Chem. Soc.* **1997**, *119*, 8566. (e) Schilstra, M. J.; Veldink, G. A.; Vliegenthart, J. F. G. *Biochemistry* **1994**, *33*, 3974. (f) Goldsmith, C. R.; Jonas, R. T.; Stack, T. D. P. *J. Am. Chem. Soc.* **2002**, *124*, 83. (g) Mayer, J. M.; Made, E. A.; Roth, J. P.; Bryant, J. R.; Matsuo, T.; Dehestani, A.; Bales, B. C.; Watson, E. J.; Osako, T.; Vallient-Saunders, K.; Lam, W. H.; Hrovat, D. A.; Borden, W. T.; Davidson, E. R. *J. Mol. Catal. A: Chem.* **2006**, *251*, 24. (h) Roth, J. P.; Yoder, J. C.; Won, T. J.; Mayer, J. M. *Science* **2001**, *294*, 2524. (i) Mayer, J. M. *Annu. Rev. Phys. Chem.* **2004**, *55*, 363. (j) Bales, B.; Brown, P.; Dehestani, A.; Mayer, J. M. *J. Am. Chem. Soc.* **2005**, *127*, 2832. (k) Meunier, B. Ed. *Biomimetic Oxidations Catalyzed by Transition Metal Complexes*; Imperial College Press: River Edge, NJ, 1999.
(23) (a) Eckert, N. A.; Vaddadi, S.; Stoian, S.; Flaschenriem, C. J.; Cundari, T. R.; Munck, E.; Holland, P. L. *Angew. Chem., Int. Ed.* **2006**, *45*, 6868. (b) Bach, T.; Korker, C. *Eur. J. Org. Chem.* **1998**, *5*, 1033. (c) Verma, A. K.; Nazif, T. N.; Achim, C.; Lee, S. C. *J. Am. Chem. Soc.* **2000**, *122*, 11013. (d) Brown, S. D.; Betley, T. A.; Peters, J. C. *J. Am. Chem. Soc.* **2003**, *125*, 322. (e) Betley, T. A.; Peters, J. C. *J. Am. Chem. Soc.* **2003**, *125*, 10782. (f) Jensen, M. P.; Mehn, N. P.; Que, L. *Angew. Chem., Int. Ed.* **2003**, *42*, 4357. (g) Brown, S. D.; Peters, J. C. *J. Am. Chem. Soc.* **2004**, *126*, 4538. (h) Bart, S. C.; Lobkovsky, E.; Bill, E.; Chirik, P. J. *J. Am. Chem. Soc.* **2006**, *128*, 5302. (i) Thyagarajan, S.; Shay, D. T.; Incarvito, C. D.; Rheingold, A. L.; Theopold, K. H. *J. Am. Chem. Soc.* **2003**, *125*, 4440. (j) Hu, X.; Meyer, K. *J. Am. Chem. Soc.* **2004**, *126*, 16322. (k) Jenkins, D. M.; Betley, T. A.; Peters, J. C. *J. Am. Chem. Soc.* **2002**, *124*, 11238. (l) Kogut, E.; Wiencko, H. L.; Zhang, L.; Cordeau, D.; Warren, T. H. *J. Am. Chem. Soc.* **2005**, *127*, 11248. (m) Mindiola, D. J.; Hillhouse, G. L. *J. Am. Chem. Soc.* **2001**, *123*, 4623. (n) Mindiola, D. J.; Hillhouse, G. L. *Chem. Commun.* **2002**, *17*, 1840. (o) Waterman, R.; Hillhouse, G. L. *J. Am. Chem. Soc.* **2003**, *125*, 13350.
(24) Au, S. M.; Huang, J. S.; Yu, W. Y.; Fung, W. H.; Che, C. M. *J. Am. Chem. Soc.* **1999**, *121*, 9120.
(25) Gunnoe, T. B. *Eur. J. Inorg. Chem.* **2007**, 1185.
(26) (a) Fulton, J. R.; Bouwkamp, M. W.; Bergman, R. G. *J. Am. Chem. Soc.* **2000**, *122*, 8799. (b) Fulton, J. R.; Sklenak, S.; Bouwkamp, M. W.; Bergman, R. G. *J. Am. Chem. Soc.* **2002**, *124*, 4722. (c) Holland, A. W.; Bergman, R. G. *J. Am. Chem. Soc.* **2002**, *124*, 14684.
(27) Fox, D. J.; Bergman, R. G. *Organometallics* **2004**, *23*, 1656.
(28) (a) Jayaprakash, K. N.; Conner, D.; Gunnoe, T. B. *Organometallics* **2001**, *20*, 5254. (b) Conner, D.; Jayaprakash, K. N.; Gunnoe, T. B.; Boyle, P. D. *Inorg. Chem.* **2002**, *41*, 3042. (c) Conner, D.; Jayaprakash, K. N.; Wells, M. B.; Manzer, S.; Gunnoe, T. B.; Boyle, P. D. *Inorg. Chem.* **2003**, *42*, 4759. (d) Feng. Y.; Gunnoe, T. B.; Grimes, T. V.; Cundari, T. R. *Organometallics* **2006**, *25*, 5456.
(29) Conner, D.; Jayaprakash, K. N.; Cundari, T. R.; Gunnoe, T. B. *Organometalics* **2004**, *23*, 2724.
(30) Zhang, J.; Gunnoe, T. B.; Petersen, J. L. *Inorg. Chem.* **2005**, *44*, 2895.
(31) Oxgaard, J.; Tenn, W. J., III; Nielsen, R. J.; Periana, R. A.; Goddard, W. A., III. *Organometallics* **2007**, *26*, 1565.

Scheme 4. Proposed Reaction Pathway for the 1,2-Addition of Benzene across M−X Bonds Studied by DFT Calculations

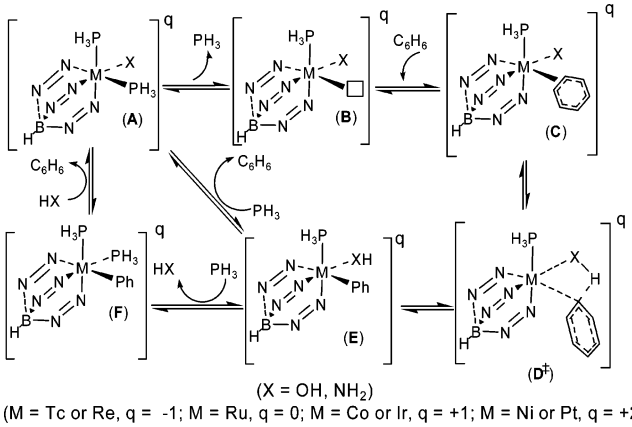

ligand in C−H bond activation,[32] and 1,2-addition of a C−H bond across a Pt−Cl bond has been implicated in Shilov-type chemistry.[9] *Thus, little is known about the various factors that impact the energetics of the 1,2-additions.* Herein, we report a comprehensive computational study that addresses the influence of the identity of the nondative ligand (OH vs NH_2) and metal [Tc(I), Re(I), Ru(II), Co(III), Ir(III), Ni(IV), and Pt(IV)] on the kinetics and thermodynamics of benzene C−H bond scission by 1,2-addition. While the present studies are specifically focused on $[(Tab)M(PH_3)X]^n$ systems, the results provide guidance for the design of systems that are more active for C−H bond activation, particularly within a catalytic cycle for hydrocarbon functionalization.

2. Computational Methods

All geometries were optimized within the Jaguar[33] program with density functional theory (DFT) using the B3LYP functional.[34] The Stevens effective core potential (ECP) and valence basis set was used,[35] with a d-polarization function on heavy main group elements (CSDZ* in Jaguar). Each structure (with exceptions as indicated) was confirmed as a minimum using an energy Hessian calculation. The *tris*-pyrazolyl borate (Tp) ligand was replaced with *tris*-azo borate (Tab), which was shown in previous work[36] to behave similarly in electronic, energetic, and steric impact to the full Tp ligand. Bader's Atoms In Molecules (AIM[37]) analysis was performed in Gaussian 03[38] using B3LYP/3-21G* (one of the largest all-electron basis sets for Ru available through EMSL[39]) with the B3LYP/CSDZ* geometries as optimized in Jaguar. An all-electron basis set is necessary to use the AIM analysis. Natural population analysis (NPA)[40] was performed in Jaguar to calculate atomic charges.

(32) Davies, D. L.; Donald, S. M. A.; Macgregor, S. A. *J. Am. Chem. Soc.* **2005**, *127*, 13754; Davies, D. L.; Donald, S. M. A.; Al-Duaij, O.; Macgregor, S. A.; Pölleth, M. *J. Am. Chem. Soc.* **2006**, *128*, 4210.
(33) Jaguar 5.5, Schrödinger, L. L. C. Portland, OR, **1991**−**2003**.
(34) Becke, A. D. *J. Chem. Phys.* **1993**, *98*, 5648.
(35) (a) Binkley, J. S.; Pople, J. A.; Hehre, W. J. *J. Am. Chem. Soc.* **1980**, *102*, 939. (b) Stevens, W. J.; Basch, H.; Krauss, M. *J. Chem. Phys.* **1984**, *81*, 6026. (c) Stevens, W. J.; Krauss, M.; Basch, H.; Jasien, P. G. *Can. J. Chem.* **1992**, *70*, 612.
(36) Bergman, R. G.; Cundari, T. R.; Gillespie, A. M.; Gunnoe, T. B.; Harman, W. D.; Klinkman, T. R.; Temple, M. D.; White, D. P. *Organometallics* **2003**, *22*, 2331.
(37) Bader, R. F. W. *Atoms in Molecules: A Quantum Theory*; Oxford University Press: Oxford, 1990.
(38) Frisch, M. J.; et al. *Gaussian 03*, revision C.02; Gaussian, Inc.: Wallingford CT, 2004.
(39) Schuchardt, K. L.; Didier, B. T.; Elsethagen, T.; Sun, L.; Gurumoorthi, V.; Chase, J.; Li, J.; Windus, T. L. *J. Chem. Inf. Model* **2007**, *47*, 1045−1052.
(40) Weinhold, F.; Landis, C. R. *Chem. Ed.: Res. Pract. Eur.* **2001**, *2*, 91.

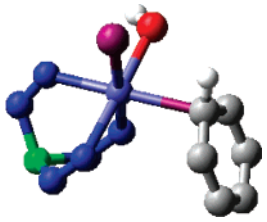

Figure 1. Calculated benzene adduct $[(Tab)Pt(PH_3)(benzene)OH]^{2+}$. All hydrogen atoms are omitted for clarity, except the hydroxo hydrogen and the hydrogen attached to the ligated carbon of benzene.

3. Results and Discussion

3.1. Structure and Bonding Considerations. We have previously reported evidence that complexes of the type $TpRu(PMe_3)_2X$ (X = OH or NHPh) initiate the 1,2-addition of aromatic C−H bonds across the Ru−X bond.[15b,c] Experimental and computational studies suggest that the transformations proceed via initial dissociation of PMe_3 and coordination of benzene to form $TpRu(PMe_3)$(benzene)X complexes, followed by C−H activation via 1,2-addition. Computational studies incorporated the smaller ligand models Tab (*tris*(azo)borate) and PH_3 in place of Tp and PMe_3, respectively. The proposed reaction pathway is depicted in Scheme 4.

We have extended computational studies of the overall benzene C−H activation shown in Scheme 4 to a series of octahedral d^6 complexes in which the identity of the metal and ligand X are varied: $[(Tab)M(PH_3)_2X]^q$ (X = OH or NH_2; M = Tc or Re, $q = -1$; M = Ru, $q = 0$; M = Co or Ir, $q = +1$; M = Ni or Pt, $q = +2$). Since Tab is a tridentate, six-electron donor ligand, complexes **A**, **C**, **E**, and **F** are formally 18-electron, six-coordinate, and octahedral (Scheme 4). Species **B**, $[(Tab)M(PH_3)X]^q$, is formally a 16-electron, five-coordinate complex. However, the π-donation capability of X can render the active species (**B**) closer to 18-electron, as judged by the planar coordination mode at the nitrogen (when X = NH_2) of the amido ligand in these complexes (see below).[41] All coordination geometries of optimized minima for complexes **A**, **E**, and **F** are as expected, and the DFT calculations present no surprises in this regard. However, structures **C** and $\mathbf{D}^{\ddagger}$, the benzene adduct and the C−H activation transition state, respectively, vary among the complexes. More detailed analysis of these systems is given below.

3.1.1. Benzene Adduct Geometries. For the overall C−H activation of benzene, the arene adducts (**C** in Scheme 4) can not only impact the rate of the overall reaction but also enhance the Arrhenius prefactor. The benzene adducts in the proposed pathway for C−H activation serve to align the substrate arene with the activating ligand X, preparing the complex for carbon−hydrogen bond activation. The pertinent complexes shall be designated briefly as $[M-X]^q$ to indicate the specific metal (M), activating ligand (X) and overall charge of the complex (q).

Benzene adducts were found for $[Ir-OH]^+$, $[Ni-OH]^{2+}$, $[Pt-OH]^{2+}$, $[Ni-NH_2]^{2+}$, and $[Pt-NH_2]^{2+}$ complexes with a representative structure shown in Figure 1 for $[(Tab)Pt(PH_3)$-(benzene)$OH]^{2+}$. In contrast, related benzene adducts were not located for $[Tc-OH]^-$, $[Re-OH]^-$, [Ru−OH], $[Co-OH]^+$, $[Tc-NH_2]^-$, $[Re-NH_2]^-$, $[Ru-NH_2]$, $[Co-NH_2]^+$ or [Ir−

(41) For all metals, in **A** the amido ligand is pyramidal, suggesting σ-only donation. In the active species **B**, however, the amido ligand is planar, allowing two-electron π-donation to satisfy the 18-electron rule.

Table 1. Representative Geometric Data for Calculated Benzene Adducts $[(Tab)M(PH_3)(benzene)X]^{q\,a}$

(Tab)M(PH$_3$)(benzene)OH				
metal	MC$_1$ (Å)	MC$_2$ (Å)	Bz C–C (Å)	Bz C–H oop (deg)
Tc	4.41	4.37	1.40	0.3
Re	4.41	4.44	1.40	0.5
Ru	3.95	4.23	1.40	1.5
Co	3.07	3.30	1.40	4.5
Ir	2.59	3.02	1.42	14.8
Ni	2.42	3.03	1.43	17.7
Pt	2.40	3.09	1.44	27.6

(Tab)M(PH$_3$)(benzene)NH$_2$				
metal	MC$_1$ (Å)	MC$_2$ (Å)	Bz C–C (Å)	Bz C–H oop (deg)
Tc	4.26	4.39	1.40	0.1
Re	4.56	4.95	1.40	0.0
Ru	5.14	5.18	1.40	0.5
Co	4.59	4.76	1.40	3.0
Ir	4.69	4.97	1.40	2.3
Ni^b	2.61	3.13	1.42	14.1
Pt	2.49	3.13	1.43	23.6

[a] C_1 and C_2 are the two benzene carbon atoms closest to the metal center. 'Bz C−H oop' is the out-of-plane bending angle of the activated H from the plane of the benzene ring. [b] A benzene adduct was located for Ni−NH_2 using a different SCF convergence algorithm (iacscf = 1 in Jaguar). At the optimized geometry, the usual SCF algorithm reports a small imaginary mode of 13i cm^{-1}.

$NH_2]^+$. With the interaction of the benzene adducts occurring to a single carbon, the calculated adducts structurally resemble intermediates expected in electrophilic aromatic substitution (EAS). In the classical EAS mechanism, an electrophile attacks a carbon of the arene ring to form an arenium intermediate, and subsequent intermolecular deprotonation restores aromaticity to yield the substituted aromatic product. In the present EAS analogy, the base for metal-mediated C−H activation is the ligand X, which serves as an intramolecular base.[42] Since this mechanism is expected to be restricted to aromatic substrates, the present mechanism may more properly be understood to be an example of internal electrophilic substitution (IES), in agreement with similar work by Oxgaard, Periana, Goddard et al.[31] This is similar in some respects to proposed C−H activation via electrophilic substitution by late transition metal complexes (with the exception that the proton transfer is generally considered an intermolecular reaction).[9]

We note that unlike previous computational studies[15b,c] of (Tab)Ru(PH$_3$)OH, an η^2-*C,C*-bound benzene adduct was not isolated in the present research, which may be a reflection of a slight downsizing of the Ru basis set (CSDZ* is valence double-ζ; previous simulations employed the full triple-ζ contraction for the Stevens' valence basis sets[35c]) or, more likely, the inherent weakness of the metal−benzene interaction in neutral complexes of this type. In a previous study of benzene C−H activation by full TpRu(L)R complexes (L = CO, PR_3 or CNH; R = alkyl or aryl),[43] it was observed that while benzene binding was weakly *exothermic*, an unfavorable entropic contribution rendered this event *endergonic*. Thus, consistent with the current calculation, the previous calculations of TpRu-methyl complexes suggests relatively weak benzene coordination. In addition, the

(42) Even for cationic complexes, benzene adducts **C** are not as strongly bound as, for example, a quintessential EAS intermediate such as protonated benzene (B3LYP/6-311++G(d,p) geometry optimization), which has a very long "Bz C−C" (1.47 Å) and large "Bz C−H oop" (30°). See Table 1 for a discussion of these metrics, and comparable $[M-X]^{q+}$ values.

(43) Foley, N. A.; Lail, M.; Lee, J. P.; Gunnoe, T. B.; Cundari, T. R.; Petersen, J. L. *J. Am. Chem. Soc.* **2007**, *129*, 6765.

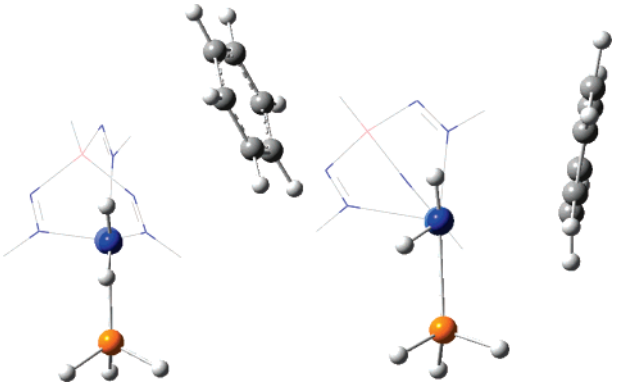

Figure 2. Benzene adducts of $[(Tab)Co(PH_3)(benzene)NH_2]^+$ (left) and $[(Tab)Ni(PH_3)(benzene)NH_2]^{2+}$ (right). The Tab ligand is shown in wire-frame for clarity. Pertinent metric data given in Table 1.

previous studies revealed that the details of the metal−benzene interaction are subtle. For example, while benzene bonding modes in TpRu(Ph)(CO)(benzene) and TpRu(Ph)(CNH)(benzene) were calculated to η^2-*C,C*, the related complex TpRu(Ph)(PMe$_3$)(benzene) showed η^2-*C,H* bonding of the benzene, which is quite similar to the adducts calculated herein, due to steric reasons.[43] Thus, given the previous subtlety of benzene coordination mode for TpRu(L)R systems, it is not surprising that coordination of benzene by $[(Tab)M(PH_3)X]^q$ is highly dependent on M and X.

Table 1 presents pertinent geometric data for calculated benzene adducts. Several structural trends as a function of metal and activating ligand are observed. Strongly bound benzene adducts only occur for cationic complexes, e.g., $[Ni-OH]^{2+}$, $[Pt-OH]^{2+}$, and $[Ir-OH]^+$ among the hydroxo complexes, and $[Pt-NH_2]^{2+}$ among the amido complexes. As expected for electrophilic addition to benzene, dicationic group 10 metal complexes show structural evidence of stronger benzene binding as compared to cationic group 9 species (e.g., compare benzene adducts of $[Ir-OH]^+$ and $[Pt-OH]^{2+}$, Table 1). The structural assessments are made primarily on the basis of the long metal−carbon(benzene) bond distances found in the congeners containing earlier (neutral or anionic) transition metal complexes, which substantially shortens for the later (cationic) complexes. Other structural indicators of greater benzene/complex interaction and activation for cationic complexes include longer C−C bond lengths for the benzene bond closest to the metal, and pyramidalization of the carbon in the proximal C−H bond (Figure 1). Such changes as a function of overall charge are expected and partly reflect the lack of solvent effects in the modeling. What is perhaps more unexpected and interesting is the role of metal (M) for a given molecular charge. Benzene binding is stronger for heavier congener within a triad (e.g. compare benzene adducts of $[Co-OH]^+$ vs $[Ir-OH]^+$ or $[Ni-NH_2]^{2+}$ vs $[Pt-NH_2]^{2+}$, Table 1).

The degree of metal−NH_2 π-interaction in the amido complexes, as well as its response to modification of the complex, is interesting and can be assessed by the "flap" angle of the amido plane (i.e., the H···H−N−M improper dihedral). When the metal−benzene interaction is very weak, the amido flap angle is close to 180°, as it is for Tc−, Re−, Ru−, Co−, and Ir−amido complexes (179° for each). Figure 2 shows the calculated geometry of species **C** for $[Co-NH_2]^+$, for which the benzene and Co essentially do not interact. The structural results for some amido complexes thus imply that there is

Table 2. Electronic Properties of 16-Electron $[(Tab)M(PH_3)(X)]^a$

	LUKSO[b] energy (au)		NPA charge on metal (e^-)	
metal	OH	NH_2	OH	NH_2
Tc	0.090	0.098	0.153	0.062
Re	0.086	0.095	0.277	0.195
Ru	−0.082	−0.072	0.330	0.233
Co	−0.283	−0.268	0.705	0.628
Ir	−0.269	−0.253	0.690	0.597
Ni	−0.502	−0.485	0.863	0.831
Pt	−0.477	−0.457	0.907	0.851

[a] Lowest unoccupied Kohn−Sham orbital (LUKSO) energies in atomic units are determined at the calculated minima of $[TabM(PH_3)(X)]$ using the B3LYP/CSDZ* level of theory. NPA = natural population analysis. [b] For comparison purposes the highest occupied Kohn−Sham orbital (HOKSO) energy of benzene at the same level of theory is −0.246 au.

significant π-donation from the amido ligand to the metal center that competes with the coordination of benzene. Alternatively, the enhanced amido-to-metal π-bonding compensates for the lack of metal−benzene bonding. The amido flap angle in those cases in which the amido is not planar is reduced toward the 109.5° value expected for σ-only bonding for $[Ni-NH_2]^{2+}$, Figure 2, and $[Pt-NH_2]^{2+}$ (123° and 116°, respectively), implying that coordination of the benzene effectively saturates the metal, thus ameliorating the degree of metal−amido dπ−pπ interaction. The foregoing comments must be tempered to some degree as planarity of a metal−amido ligand may also arise in the limit of a significantly ionic ($L_nM^+NH_2^-$) bonding description.[44]

Investigation of the electronic structure of benzene adducts (**C** in Scheme 4) reveals an increasing interaction between the metal and benzene as the acidity of the metal increases. The acidity of 16-electron complex **B** was assessed using the LUKSO (lowest unoccupied Kohn−Sham orbital[45]) energy and NPA charge on the metal. A lower LUKSO energy and a more positive NPA charge imply a more acidic metal center. Since NH_2^- is a stronger base than OH^- (based on gas-phase proton affinities[46]), we expect the metal center to be less acidic for the amido complexes as compared to the hydroxo complexes, and indeed this is the case. For each hydroxo species **B**, the corresponding amido species is calculated to be less acidic as indicated by the LUKSO energies and NPA charge on the metal, Table 2.

For both the hydroxo and amido systems containing Tc, Re, and Ru, no benzene adducts were found via DFT geometry optimization. The HOKSO (highest occupied Kohn−Sham orbital) energy of benzene at the level of theory used is −0.246 a.u. Analysis of LUKSO energies in Table 2 indicates that benzene binds only in the limit that $\epsilon_{LUKSO}([M-X]^q) < \epsilon_{HOKSO}$-(benzene), supporting the conclusion made above as to the correlation between the acidity of **B** and its ability to form a stable adduct **C**. Caution is needed, however, in interpretation of the present results, as experiments are conducted in condensed media. The overall charge of the complex is an obvious factor in regulating the interaction between the active species **B** and benzene. In the absence of solvation, charge effects will dominate. However, the comparison of NPA and LUKSO data in Table 2 for systems with equivalent charge make it apparent that both M and X can modify the acidity/basicity of **B** and thus provide evidence for the important electronic role that the metal M and the ligand X play in modifying the overall activity toward C−H bond cleavage.

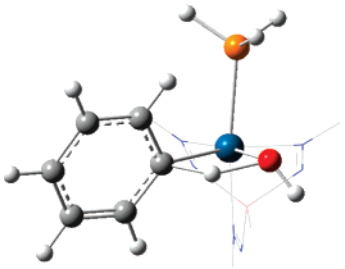

Figure 3. Calculated transition state for C−H activation of benzene by $[(Tab)Pt(PH_3)OH]^{2+}$. Tab ligand is shown in wireframe.

3.1.2. Transition States for Benzene C−H Activation. As expected from previous studies by our group and others,[13,15,36] the transition states (TSs) for C−H bond activation of benzene by the M−X bond of $[(Tab)M(PH_3)(benzene)X]^q$ have a four-centered arrangement with a kite-shaped geometry resulting from the obtuse angle about the hydrogen being transferred. The imaginary frequencies in these transition states correspond almost exclusively to C···H and X···H bond-forming/-breaking via motion of the active hydrogen. The TS structure results in a relatively short metal−hydrogen distance since the M···C and M···X distances in such transition states are typically only marginally longer (∼10−20%) than normal covalent bond lengths. A representative example of the calculated transition state for benzene C−H activation by $[(Tab)Pt(PH_3)OH]^{2+}$ is shown in Figure 3. In these transition states the benzene ring is more or less perpendicular to the plane defined by the X···M···C···H ring.

Short M···H distances in SBM transition states have been used in the past as a gauge of metal−hydrogen interaction.[47] For the systems studied herein, the "reduced" M−H distances (calculated by subtracting the sum of the covalent radii[48] of the metal and hydrogen from the M···H distance in transition state $\mathbf{D}^{\ddagger}$) were calculated. A plot of this metric is given in Figure 4, showing the metric as a function of metal and ligand X. In relative terms, the M···H "bond" in the transition states are on average 8% longer than covalent estimates in the hydroxo systems and 12% longer in the amido complexes, which could be taken as an indicator of significant bonding between the metal and the hydrogen of the C−H bond being activated. However, a metric analysis may be too simplistic as there must also be electron density along the internuclear axis.

To analyze the nature of the bonding in the transition state, Atoms in Molecules[37] (AIM) analyses were performed for representative [Ru−OH] and $[Ru-NH_2]$ benzene C−H activation transition states. The AIM technique is a topological analysis of the calculated electronic structure of a molecule, which, among other procedures, searches for critical points (stationary points) in the total electron density. Such critical points are taken to indicate that bonding exists among two or

(44) Grotjahn, D. B.; Sheridan, P. M.; Jihad, I. A.; Ziurys, L. M. *J. Am. Chem. Soc.* **2001**, *123*, 5489.
(45) Kohn-Sham orbitals, e.g., frontier orbitals HOKSO and LUKSO, are the DFT equivalent of molecular orbitals and may be similarly interpreted.
(46) Linstrom, P. J., Mallard, W. G. Eds. *NIST Chemistry WebBook, NIST Standard Reference Database Number 69*; National Institute of Standards and Technology: Gaithersburg MD, 2005; 20899 (http://webbook.nist.gov).
(47) See, for example: Cundari, T. R.; Gordon, M. S. *J. Am. Chem. Soc.* **1993**, *115*, 4210.
(48) WebElements Scholar, http://www.webelements.com/, accessed January 2007.

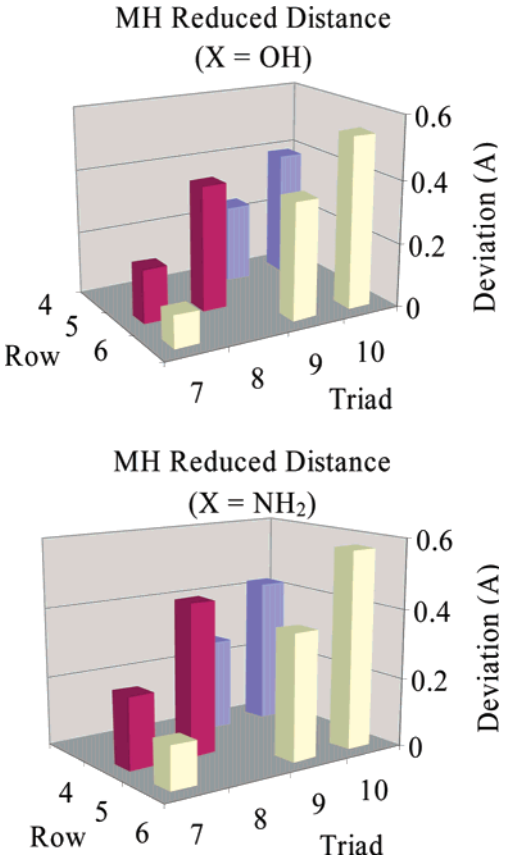

Figure 4. Reduced M−H bond distance (i.e., M···H distance in transition state minus sum of covalent radii of metal and hydrogen) by row and group and by X group.

Scheme 5. Two Possible Depictions from Atoms in Molecules (AIM) Analyses for Benzene CH Activation Transition States[a]

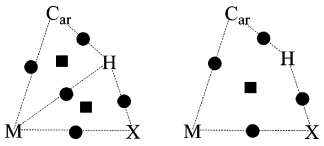

[a] Square indicates a ring critical point; a circle indicates a bond critical point. The AIM analysis is more consistent with the depiction on the right for [Ru−OH] and [Ru−NH_2] transition states.

more atoms. The AIM analysis indicates four bond critical points (M···X, X···H, C···H, and M···C), thus implying a M···X···H···C four-membered ring, which is confirmed by the identification of a ring critical point in the electron density within the proposed cycle. No bond critical point could be located between the X···C pairs. What is more intriguing is that the AIM analysis does not indicate a bond critical point between the metal and hydrogen in the active site of the transition state. Hence, the bond connectivity in Scheme 5 (right) is suggested for these transition states. In the limit of a M···H bond, one would also expect two ring critical points for the individual three-membered cycles (Scheme 5, left).

The OHM description is thus contraindicated for these transition states on the basis of the lack of significant M−H interaction as determined by the AIM analysis. In considering the nature of the transition state for C−H activation, a useful comparison can be made between the SBM transition state indicated by the AIM analysis and IES (see above) mechanism. The major difference between SBM and IES is the participation of the lone pair on the ligand "X" in the C−H activation step.

Scheme 6. Calculated Metric Data for C−H Activation of Benzene by TabRu(PH_3)(X), where X = CH_3,[49] NH_2, or OH

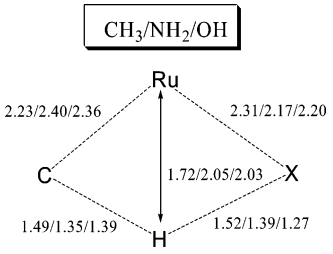

Table 3. Early vs Late CH Activation Transition States[a]

	X = OH			X = NH_2		
metal	*D*(C···H) (%)	*D*(O···H) (%)	TS type	*D*(C···H) (%)	Δ(N···H) (%)	TS type
Tc	27	10	late	23	19	late
Re	24	13	late	21	21	middle
Ru	22	15	late	19	23	middle
Co	19	18	middle	14	28	early
Ir	22	18	middle	13	32	early
Ni	15	22	early	12	31	early
Pt	15	25	early	11	36	early

[a] Δ(C···H) or Δ(X···H) is the calculated percent lengthening of the particular bond in the transition state versus typical covalent single bond lengths.

We have previously suggested the role of the lone pair for activation of dihydrogen and intramolecular C−H activation by (PCP)Ru(CO)NH_2.[29] Scheme 6 provides a comparison of the calculated distances for the four atoms that compose the active site for benzene C−H activation by (Tab)Ru(PH_3)(C_6H_6)X for X = CH_3,[15c,49] NH_2, and OH. It is readily apparent from the metric data that the X groups with a lone pair (NH_2 and OH) are quite similar to each other, while the methyl-activating ligand is more disparate. Thus, the metric data for the calculated transition states indicate a substantial difference between X = Me and X = OH/NH_2. The origin of this difference is likely the presence of a lone pair on the amido and hydroxo ligands. What is particularly noticeable is the much shorter Ru···H distance in the transition state for X = CH_3. We propose that the directed sp^3 hybrid of the methyl-activating ligand less effectively "bridges" *both* the transfer hydrogen and the metal, and thus must compromise binding with each of these moieties. As a result, the Ru−X−H angle is small and the resulting Ru···H distance short. Bercaw et al. presented a similar analysis for the preference of H over alkyl for the transfer group in their classic study of SBM by scandium−alkyl complexes.[14] For complexes with amido- and hydroxo-activating ligands, the presence of available lone pairs makes these ligands more effective at "bridging" M and H, and thus the Ru−X−H angle can expand, and Ru···H can be longer, as depicted in Scheme 6.

As a measure of the relative position of the transition state on the reaction coordinate (i.e., early versus late transition states), the percent deviations from a typical single C−H and X−H bond length (as determined by the sum of covalent radii) for both hydroxo and amido ligands are presented in Table 3. Inspection of the data in Table 3 indicates that the transition

(49) Lail, M.; Bell, C. M.; Cundari, T. R.; Conner, D.; Gunnoe, T. B.; Petersen, J. L. *Organometallics* **2004**, *23*, 5007.

states are late for structures with electron-rich (anionic) metal centers (e.g., $[Tc-OH]^-$, $[Re-OH]^-$, and $[Tc-NH_2]^-$) and become progressively earlier for more acidic (cationic) metal centers. The calculations are consistent with more electron-rich metal centers being more efficient at promoting the donation of electron density into the C−H σ^* orbital, causing a longer (later) C−H bond length in the transition state.[12] The amido transition states are relatively early as compared to those of their hydroxo congeners, Table 3, which is expected of the more basic amido ligand under the IES mechanism.

One might ask why oxidative hydrogen migration was observed as the mechanism in similar systems[14b,15,49,50] but not here. The ligand receiving the transferred hydrogen is an alkyl group in systems showing OHM as a mechanism (e.g., (Tab)-Ru(L)(C_6H_6)R), but the current research employs heteroatomic hydroxo and amido as the activating ligands. The most obvious difference between these X groups is the existence of lone pairs on the hydroxo and amido ligands that are missing in the alkyl systems. Indeed, an AIM analysis of the X = CH_3 transition state lacks a four-membered ring critical point and instead indicates true Ru−H(*ipso*) interaction as prescribed by the OHM mechanism. It is reasonable that rather than a metal dπ orbital,[12] perhaps an available lone pair on X is responsible for the donation of electron density to the activated hydrogen.[12] That is, when the ligand X possesses a lone pair, it functions as an intramolecular base, which is consistent with the IES mechanism and highlights a fundamental difference between heteroatom- and hydrocarbyl-activating ligands. In fact, on the basis of this premise, we suggest that SBM/IES type C−H activation might be inherently more facile when the "receiving ligand" is anionic and heteroatomic than for hydrocarbyl ligands. Future efforts will address this issue in more detail. To assess the role of the X group using metric data, the M−X bond lengths from the active species (**B**), the transition states (**D**‡), and products (**E**) are compared. If the donation to σ^*_{CH} is primarily from the ligand, the M−X bond length in the transition state is expected to more closely resemble the product. Conversely, if the donation to σ^*_{CH} is primarily from the metal center (i.e., substantial M−H interaction), we propose that the transition state M−X bond length should be no greater than halfway between the corresponding values calculated for **B** and **E**. In all cases, the M−X bond lengths in the transition states are closest to the product values (Table 4) on average 64% for hydroxo and 70% for amido, a structural indicator of a more significant contribution to C−H bond scission from the ligand than the metal.

These results suggest that the mechanism for C−H activation by $[(Tab)M(PH_3)X]^n$ fragments (where X = a formally anionic heteroatomic ligand such as hydroxo or amido) is perhaps best viewed as an intramolecular proton transfer or IES as defined by Goddard, Periana, et al. (Scheme 7).[31] An important mechanistic distinction between IES and an aromatic substitution is based on the interaction of the metal with the C−H bond rather than the arene π-system. Upon coordination to the metal center, acidic character is imparted to the C−H bond, resulting in relatively facile proton transfer to the basic ligand "X." Calculated results for the transition state of benzene C−H activation that are consistent with the intramolecular proton-transfer view include: (1) shorter Ru−H bond distance for X = Me than for X = OH or NH_2, (2) shorter M−H bond distances for less basic OH ligands than for NH_2 ligands, and (3) longer M−H bond distances for later and more electrophilic metals (Figure 4). Such a reaction is similar to net heterolytic cleavage of dihydrogen by transition metal−amido complexes and has been previously discussed for intramolecular C−H activation by a Ru(II) parent amido system.[25,29,51] In addition, related mechanistic issues and conclusions have been discussed recently in an excellent detailed computational analysis including an interesting explicit investigation of orbital transformations involved in C−H activation by an Ir(III)−methoxo complex.[31]

Table 4. Comparison of M−X Bond Lengths (Å) between the Active Species, Transition State, and Product[a]

metal	X	active species (**B**)	transition state (**D**‡)	product (**E**)	percent completion
Tc	OH	2.03	2.30	2.44	66
Re	OH	2.00	2.28	2.40	68
Ru	OH	1.97	2.20	2.30	69
Co	OH	1.77	1.94	2.06	60
Ir	OH	1.92	2.15	2.23	75
Ni	OH	1.76	1.92	2.07	53
Pt	OH	1.92	2.11	2.25	58
Tc	NH_2	2.01	2.23	2.31	75
Re	NH_2	1.99	2.21	2.29	75
Ru	NH_2	1.95	2.17	2.25	74
Co	NH_2	1.77	1.95	2.05	66
Ir	NH_2	1.95	2.12	2.19	70
Ni	NH_2	1.77	1.95	2.05	63
Pt	NH_2	1.91	2.11	2.20	69

[a] Percent completion is the ratio of the transition-state bond length to the product bond length, relative to the active species' bond length, e.g., 50% completion means the transition-state bond length is exactly halfway between the active species and product bond lengths.

Scheme 7. Proposed Mechanism for C−H Activation by $[(Tab)M(PH_3)(C_6H_6)X]^n$ (X = OH or NH_2) Is Best Described as an Intramolecular Proton Transfer

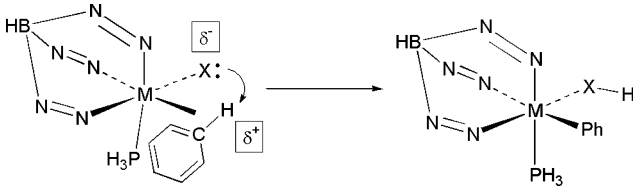

3.2. Kinetic and Thermodynamic Considerations. Analysis of the structural and electronic properties of the various stationary points along the reaction pathway for 1,2-addition of the C−H bond of benzene has revealed a considerable degree of sensitivity to modification of the metal, including overall complex charge and the activating ligand X. It is also likely that exchange of the phosphine ligand (PH_3 for the calculations) also influences the energetics of C−H activation.[43] From the perspective of rational design of activating complexes, this flexibility is highly desirable as it suggests considerable ability to tune d^6 TpM(L)X complexes toward optimal activity and selectivity. Attention is now turned to issues of kinetics and

(50) (a) Oxgaard, J.; Periana, R. A.; Goddard, W. A., III. *J. Am. Chem. Soc.* **2004**, *126*, 11658. (b) Oxgaard, J.; Goddard, W. A., III. *J. Am. Chem. Soc.* **2004**, *126*, 442.

(51) (a) Sandoval, C. A.; Ohkuma, T.; Muniz, K.; Noyori, R. *J. Am. Chem. Soc.* **2003**, *125*, 13490. (b) Murata, K.; Konishi, H.; Ito, M.; Ikariya, T.; *Organometallics* **2002**, *21*, 253. (c) Guo, R.; Morris, R. H.; Song, D. *J. Am. Chem. Soc.* **2005**, *127*, 516. (d) Clapham, S. E.; Hadzovic, A.; Morris, R. H. *Coord. Chem. Rev.* **2004**, *248*, 2201. (e) Abdur-Rashid, K.; Clapham, S. E.; Hadzovic, A.; Harvey, J. N.; Lough, A. J.; Morris, R. H. *J. Am. Chem. Soc.* **2002**, *124*, 15104. (f) Abdur-Rashid, K.; Faatz, M.; Lough, A. J.; Morris, R. H. *J. Am. Chem. Soc.* **2001**, *123*, 7473. (g) Heiden, Z. M.; Rauchfuss, T. B. *J. Am. Chem. Soc.* **2006**, *128*, 13048. (h) Fryzuk, M. D.; Montgomery, C. D.; Rettig, S. J. *Organometallics* **1991**, *10*, 467.

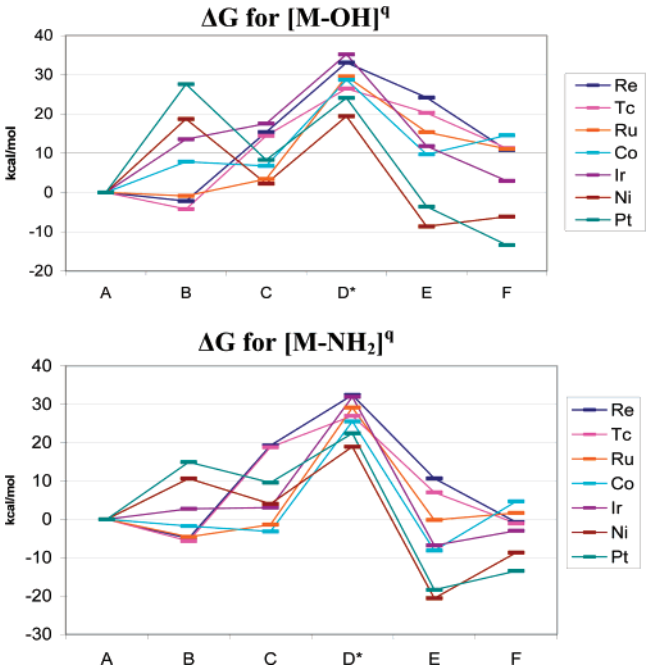

Figure 5. Calculated ΔG for benzene C−H activation by the complexes (Tab)M(PH_3)$_2$X for X = OH (top) and X = NH_2 (bottom). D* represents the transition state for C−H activation.

thermodynamics to probe whether the calculated molecular and electronic structural changes discussed above are manifested in the energetics of C−H bond activation of benzene by the model scorpionate complexes.

An overview of the proposed reaction pathway for benzene C−H activation is given in Scheme 4. The overall transformation involves the loss of phosphine from the 18-electron precursor [(Tab)M(PH_3)$_2$X]^q (**A**) to generate the formally 16-electron species [(Tab)M(PH_3)X]^q (**B**). Benzene then coordinates to **B** to form the adduct [(Tab)M(PH_3)(benzene)X]^q (**C**), which is followed by the transition state for benzene C−H activation (**D**‡) leading to 18-electron product (Tab)M(HX)(PH_3)(Ph) (**E**). The dative ligand XH may then be replaced by the original PH_3 to yield *bis*-phosphine complex (Tab)M(PH_3)$_2$(Ph) (**F**).[15b,c] Calculated free energies for these steps are depicted in Figure 5 for [M−OH]^q (top) and [M−NH_2]^q (bottom) complexes.

Three thermodynamic criteria were used to assess the suitability of different metal−ligand combinations for C−H bond activation of benzene. The first criterion we evaluated is the energetic barrier to the formation of the unsaturated species **B** from the precursor **A**, as C−H activation of benzene requires coordination to the metal center. Second, the magnitude of the benzene C−H activation transition state **D**‡ relative to starting materials **A** is considered. The third criterion assessed here is the thermoneutrality of the proton-transfer step (**B** + PhH → **E**), which is related to incorporation of the C−H activation sequence into potential catalytic cycles. For efficient catalysis, this reaction should be close to thermoneutral in order to avoid thermodynamic "sinks."

3.2.1. Generation of 16-Electron Active Species. The generation of the active species **B** plays an obviously important role in determining the overall rate of benzene C−H activation. If the unsaturated complex is too high in energy, activation of the C−H bond will be hampered by a low concentration of active species **B** or, alternatively, require a larger concentration

Table 5. Free Energies (kcal/mol) for Generation of 16-Electron Active Species [(Tab)M(PH_3)X]^q (**B**) from [(Tab)M(PH_3)$_2$X]^q (**A**)[a]

M	X = OH	X = NH_2	M	X = OH	X = NH_2
Tc	−4.2	−5.7	Ir	13.6	2.8
Re	−2.2	−5.0	Ni	18.7	10.6
Ru	−0.9	−4.6	Pt	27.6	14.9
Co	7.8	−1.8			

[a] This is the B3LYP/CSDZ* calculated free energy for the reaction, TabM(X)(PH_3)$_2$ → TabM(X)(PH_3) + PH_3.

Table 6. Free Energies (kcal/mol) of Activation of Benzene C−H Bond Starting from (Tab)M(PH_3)$_2$X (**A**)[a]

M	X = OH	X = NH_2	M	X = OH	X = NH_2
Tc	26.5	27.0	Ir	35.2	32.0
Re	33.0	32.4	Ni	19.4	18.9
Ru	29.6	29.1	Pt	24.1	22.4
Co	28.7	25.5			

[a] This is the B3LYP/CSDZ* calculated free energy difference between transition state **D**‡ and reactants **A**.

of the precursor complex **A**. The free energies to create the 16-electron active species are given in Table 5. In general, the extrusion of phosphine becomes more endergonic as the charge on the complex becomes more positive, which is consistent with tighter binding of the Lewis basic phosphine to a more acidic metal center. However, given the favorable entropy for a bond dissociation process, the overall $\Delta G_{bind}(PH_3)$ for this step is not inordinate for any complex, being less than 28 kcal/mol for even the most tightly bound system, [Pt−OH]$^{2+}$, and much less than this for all other complexes studied.

Phosphine loss is more favorable for the amido complexes than for their hydroxo counterparts, suggesting an advantage for the former in the way of a greater concentration of active species for [M−NH_2] than for the corresponding [M−OH] complexes. We hypothesize that this difference is a consequence of greater π-donation for the amido ligands versus hydroxo ligands, as discussed above, which nominally puts the active species closer to a more stable 18-electron count. Hence, from the perspective of generation of 16-electron active species **B**, amido complexes are expected to have an advantage over their hydroxo counterparts.[52]

3.2.2. Kinetic Barrier to C−H Bond Activation of Benzene. In terms of targeting new systems capable of facile C−H activation via 1,2-addition across M−X bonds, the most pertinent energetic parameter is the activation barrier for the C−H bond-breaking event. For convenience and ease of comparison, we have defined this barrier as the calculated free energy difference between the precursor complex (Tab)M(PH_3)$_2$X (**A**) and the transition states (**D**‡, Table 6).

The transition states for benzene C−H activation, **D**‡, fall within the free energy range of ~19 kcal/mol ([Ni−X]$^{2+}$ for X = OH, NH_2) to ~35 kcal/mol ([Ir−OH]$^+$) above precursors **A**. For systems with the same total charge, progressing from a first or second row transition metal to the third row is calculated to increase the barrier to benzene C−H activation. For example,

(52) In some cases, the loss of phosphine is calculated to have a slightly favorable change in Gibbs free energy due to entropic factors. Since these are gas-phase calculations, the effects of entropy in the dissociation step are magnified beyond what is expected in solvent. However, the contribution of $T\Delta S$ is roughly constant (within 1.8 kcal/mol) across all metals for this step. Further, the entropic contribution to the **A**→**B** and **B**→**C** steps roughly cancel each other (within 4.5 kcal/mol), and the remaining steps are unimolecular, effectively eliminating solvation concerns for the purposes of this study.

Table 7. Free Energies (kcal/mol) of Hydrogen Transfer[a]

M	X = OH	X = NH_2	M	X = OH	X = NH_2
Tc	24.5	12.7	Ir	−1.7	−9.6
Re	26.4	15.6	Ni	−27.4	−31.2
Ru	16.2	4.4	Pt	−31.2	−33.3
Co	1.9	−6.4			

[a] This is the B3LYP/CSDZ* calculated free energy difference between active species **B** plus benzene and 18-electron product **E**, TabM(HX)(PH_3)(Ph).

the free energies of activation for the heavier rhenium complexes are ~6 kcal/mol higher than those of the lighter technetium congeners. Likewise, there is an increase in free energy of activation for Ir as compared to that for Co by 6.5 kcal/mol (for both X = OH and NH_2) and also platinum versus nickel (difference of 4.7 kcal/mol for X = OH and 3.5 kcal/mol for X = NH_2).

With one exception (Tc), the calculated barriers for the amido complexes are lower than those for their hydroxo counterparts by an average of 1.6 kcal/mol for the remaining six systems. The largest calculated difference is 3.2 kcal/mol for the Co and Ir systems, while the smallest magnitude difference is 0.5 kcal/mol for Tc and Ni. The magnitude of the free energy change for **A** → **D**‡ is smaller for variation of X than the change due to variation of metal (same ligand X) within a triad. Computational studies of 1,2-addition of a C−H bond of methane across the Ir−X (X = OH, OMe, OCF_3, or NH_2) bond of the model complexes Ir(Me)$_2$(NH_3)$_2$(X)(CH_4) reveal a difference in $\Delta H^{\ddagger}$ that is less than 2 kcal/mol for variation of X, which is similar in magnitude to our calculated differences upon variation of X for (Tab)M complexes.[31] However, our comparison of activation barriers for hydroxo versus those for amido are for *overall reactions* that involve phosphine dissociation, benzene coordination, and the C−H activation step. For a more direct comparison to the results for Ir(Me)$_2$(NH_3)$_2$(X)(CH_4) systems, we compared the $\Delta\Delta G^{\ddagger}$ for 1,2-addition of the C−H bond of benzene starting from [(Tab)Ir(PH_3)(C_6H_6)X]$^+$complexes. The $\Delta G^{\ddagger}$ for the 1,2-addition is 17.6 kcal/mol for X = OH and 28.9 kcal/mol for X = NH_2. Thus, we calculate a much more substantial change in activation barrier upon substitution of OH with NH_2 for (Tab)-Ir(PH_3)(C_6H_6)X systems with $\Delta\Delta G^{\ddagger}$ = 11.3 kcal/mol [compared to ≤2 kcal/mol difference for Ir(Me)$_2$(NH_3)$_2$(X)(CH_4)]. In part, these differences may reflect the impact of gas-phase calculations that incorporate entropy (this study) versus changes in enthalpy (previous study of Ir system[31]). *Combined with the structural evidence discussed above, the calculations yield an emerging picture that catalysis will be significantly influenced by both the metal M and the activating ligand X.*

3.2.3. Thermoneutrality of Hydrogen Transfer. For the possible incorporation of the C−H activation sequences into catalytic cycles, the overall thermodynamics of the hydrogen-transfer step (i.e., ΔG_{trans}, the free energy of the reaction (Tab)M-(PH_3)X [**B**] +PhH → (Tab)M(PH_3)(HX)Ph [**E**]) are important. Effective catalysis implies that these transformations be neither too favorable nor too unfavorable, as indicated in previous theory−experiment investigations of the observed efficient H/D exchange.[15c] The Ni, Pt, and Ir complexes for both activating ligands X and the Co−amido complex are exergonic for the conversion of **B** plus benzene to **E** (Table 7), implying these metals may be prime candidates for direct observation of benzene C−H activation and functionalization. Consistent with our calculations, Periana et al. have observed the conversion of an Ir(III)−methoxo complex and benzene to methanol and the corresponding Ir(III)−phenyl system.[15a] However, for the Ni and Pt model systems, the benzene C−H activations are calculated to be highly exergonic, implying that these systems *may* be less suitable for incorporation into catalytic sequences. The systems for which the **B** → **E** transformation are calculated to be closest to thermoneutral are the [Co−OH]$^+$ and [Ir− OH]$^+$ complexes.

For a given metal, the amido ligand lowers ΔG for conversion of [(Tab)M(PH_3)X]^q (**B**) plus benzene to [(Tab)M(PH_3)(XH)-Ph]^q (**E**), the free energy change for the hydrogen-transfer step, in comparison to the hydroxo ligand. The differences in Gibbs free energy range from 12.8 kcal/mol for Tc to 2.1 kcal/mol for Pt. In general, the difference between hydroxo and amido decreases from left to right in the transition series.[53]

4. Summary, Conclusion, and Prospectus

The feasibility and kinetic accessibility of the C−H activation step in a catalytic cycle like that shown on the right side of Scheme 2 have been demonstrated (at least for benzene activation) using Ru and Ir complexes.[13,15] Although much remains to be learned about these transformations, it can now be said that such reactions are accessible with late transition metal systems and that the activation barriers for C−H activation are reasonably low for implementation into catalytic cycles. The second key step, net oxygen atom insertion into an M−R or M−Ar bond, is at least equally challenging. Despite the utility and interest in these reactions, insertion of oxygen into metal−alkyl or −aryl functionalities has rarely been directly observed.[20,21] Mayer and Brown have reported the conversion of Re(VII)−oxo complexes with phenyl ligands to the corresponding phenoxo complexes, and in at least one case the transformation occurs under thermal conditions.[20] More recently, Periana et al. have reported the reaction of methylrheniumtrioxo with external oxidants (e.g., hydrogen peroxide, pyridine-*N*-oxide, periodate, and iodosyl benzene) to form Re(OMe)O_3.[21] Importantly, these transformations occur relatively rapidly at room temperature, and preliminary mechanistic studies indicate that the oxygen atom in the final methoxo ligand does not originate from a Re-oxo moiety. A mechanism similar to the classic Baeyer−Villiger organic reaction[54] has been proposed.

Thus, the two key steps in the catalytic cycle depicted on the right side of Scheme 2 have been observed; however, the C−H activations have been observed for systems with high d-electron counts [i.e., d^6 for Ru(II) and Ir(III)],[13,15] while the transformation of M−R into M−OR have only been observed for systems in high oxidation states (and thus low d-electron counts).[20,21] For the present models we have kept the d-electron count fixed at six, which has necessitated variation of the overall charge. While the precise relationship between the kinetics and thermodynamics of these transformations *vis-à-vis* d-electron counts and metal formal oxidation states is not entirely understood, it is reasonable to expect that a marriage of these two transformations may require a catalyst that satisfies both requirements (such as Co^{III}, Pt^{IV}, etc.).

(53) For example, the average difference is 11.8 kcal/mol for group 7, 11.8 kcal/mol for group 8, 8.1 kcal/mol for group 9, and 2.9 kcal/mol for group 10.

(54) Brink, G. J.; Arends, I. W. C. E.; Sheldon, R. A. *Chem. Rev.* **2004**, *104*, 4105.

Tables 5−7 provide a comparison of the three criteria considered to quantify the efficacy of (Tab)M complexes toward C−H activation and their possible use as catalysts (i.e., generation of the active species, overall hydrogen-transfer barrier, and thermoneutrality of the hydrogen-transfer step) for hydrocarbon functionalization. As expected, generation of the coordinatively unsaturated species $[(Tab)M(PH_3)X]^q$ (**B**) via loss of phosphine from the 18-electron precursors **A** becomes less favorable as the effective charge on the metal complex becomes more positive. As the charge on the metal complex becomes more positive, $\Delta G^{\ddagger}$ (**A** + PhH → **D**‡) and ΔG (**B** + PhH → **E**) for C−H activation step are both reduced (i.e., become more favorable). However, the present calculations suggest that the metal plays a primary role in the kinetic and thermodynamic feasibility of arene C−H bond activation and functionalization.

In addition to the identity of the metal, the ligand X impacts the calculated reaction energetics.[55] Pt is the metal most "tunable" by the ligand X, with a mean absolute change of 11.5 kcal/mol in ΔG due to change of ligand "X." On average, the generation of the 16-electron active species **B** from **A** by phosphine loss is ∼7 kcal/mol more facile for the amido than their hydroxo congeners, Table 5. Likewise, the **A** + PhH → **D**‡ activation barriers are ∼1−3 kcal/mol lower for X = NH_2 than X = OH. Both of these observations suggest an advantage for amido over hydroxo complexes. It is interesting to note that the energetic discrepancy between hydroxo and amido complexes becomes greater for these two criteria as one moves from left to right in the transition series. For the thermoneutrality (of hydrogen transfer) criterion, hydroxo and amido complexes are comparable in a global sense, with the early metals being closer to thermoneutral for the amido than the hydroxo complexes and vice versa for the later metal models.

Here it should be noted that, while the C−H activation step is important and is the RDS for most calculated systems, the energetics of PH_3/benzene exchange is also a potentially significant contributor to the success of C−H activation. This underscores the point that hydrocarbon coordination is often as challenging as the actual C−H bond cleavage step. Thus, when considering the impact of variation of the ligand "X," the influence on hydrocarbon coordination should also be considered, especially when varying "X" from alkyl or aryl to π-donor heteroatomic ligands such as OR or NHR, which can impact ligand coordination dramatically. For example, the complexes $TpRu(PMe_3)_2X$ (X = OPh, OH or NHPh) exhibit more rapid rates of dissociative phosphine exchange compared to $TpRu(PMe_3)_2R$ (R = Ph or Me).[15c]

A simple linear catalyst scoring function can be constructed using the calculated ΔG values for the three criteria enumerated above (see Tables 5−7) to suggest a good balance between competing catalytic trends.[56] Assigning a lower priority to the free energy of formation for the active species (**A** → **B**)[57] indicates $[Co-OH]^+$, $[Ir-OH]^+$, $[Ru-NH_2]$, $[Co-NH_2]^+$, and $[Ir-NH_2]^+$ are the best candidates for further experimental study, i.e., they have the lowest catalyst scores. It is worth noting that the catalyst scoring function is robust in that the top candidates did not change upon variation of the weights over a reasonable range of values. *Moreover, it is interesting to note that the catalyst scoring function independently arrives at models of two heavily studied and successful hydroarylation catalysts, i.e., Ru(II) and Ir(III) complexes.*[13,15] These candidates have free energies to formation of the active species less than 10 kcal/mol (except $[Ir-OH]^+$, which has a barrier of 14 kcal/mol), overall barriers to C−H activation (**A** → **D**‡) of less than 30 kcal/mol (except $[Ru-NH_2]$, with a value of 34 cal/mol due to the stability of **B**), and are thermoneutral in the hydrogen-transfer step to within 10 kcal/mol. The Co and Ir species have the additional advantage of forming reasonable benzene adducts, leading to enhancement in the Arrhenius prefactor for the hydrogen-transfer step. It is also interesting to note that none of these candidates exhibit a late transition state structure (see Table 3). Among all the candidates, $[Co-OH]^+$ has the most favorable "score"[56,57] and appears to be the most promising for further research and tuning to optimize the potential catalytic activity on the basis of an accessible barrier to hydrogen transfer (21 kcal/mol), near thermoneutrality for hydrogen transfer (+2 kcal/mol), and small barrier to formation of the active species (8 kcal/mol).

The AIM analysis as well as calculated structural metrics and energy barriers implicates a fundamental shift in the nature of the bonding in the transition state upon going from an X with no available lone pairs (i.e., X = methyl) to heteroatom X groups with available lone pairs such as OH and NH_2. We propose that, while the mechanism of C−H activation for X = hydrocarbyl is more akin to an OHM/SBM description, the transition states for X = OH, NH_2 more closely resemble those envisaged for Shilov-type systems in which hydrogen transfer is an intramolecular process. In terms of development, X = heteroatom systems may provide more profitable systems for design and fine-tuning of hydrocarbon functional catalysts, generally, and hydroarylation catalysts, specifically. Indeed, such integrated theory−experiment studies are underway in our research laboratories.

Acknowledgment. T.B.G. acknowledges the National Science Foundation (CAREER Award; CHE 0238167) and the Alfred P. Sloan Foundation (Research Fellowship) for financial support of this research. T.R.C. acknowledges the U.S. Department of Education for its support of the CASCaM facility. The research at UNT was supported in part by a grant from the Offices of Basic Energy Sciences, U.S. Department of Energy (Grants No. DEFG02-03ER15387). Calculations employed the UNT computational chemistry resource, which is supported by the NSF through Grant CHE-0342824.

Supporting Information Available: Details of calculated stationary points; the complete citation for ref 38 (listed as ref 6 for Supporting Information refs). This material is available free of charge via the Internet at http://pubs.acs.org.

JA074125G

(55) For each step, the average range of free energy values is ca. 20 kcal/mol (holding the ligand constant, for both ligands), whereas the range of the *difference* between the two ligands for each step (i.e., holding the metal constant) is ca. 13 kcal/mol, only 65% of the variation due to the metal.

(56) The weighted sum of the ΔG values of the corresponding criteria may be combined to produce a score, $S = w_{act}\Delta G_{act} + w_{barrier}\Delta G_{barrier} + w_{xfer}|\Delta G_{xfer}|$, with lower scores being more desirable (see Tables 5−7 for ΔG values).

(57) Specifically, $w_{act} = 1$ and $w_{barrier} = w_{xfer} = 2$.